Veterinary Microbiology 233 (2019) 85–92

Contents lists available at ScienceDirect

Veterinary Microbiology

journal homepage: www.elsevier.com/locate/vetmic

Changes in the small intestine mucosal immune barrier in Muscovy ducklings infected with Muscovy duck reovirus

Yijian Wu[a,b,1], Zhenni Liu[a,1], Erpeng Zhu[c], Minghui Li[a], Huihui Jiang[a], Yu Luo[a], Quanxi Wang[a,b], Xiaoping Wu[a,b], Baocheng Wu[a,b], Yifan Huang[a,b,*]

[a] College of Animal Science, Fujian Agriculture and Forestry University, Fuzhou 350002, People's Republic of China
[b] Fujian Key Laboratory of Traditional Chinese Veterinary Medicine and Animal Health, Fujian Agricultural and Forestry University, Fuzhou 350002, People's Republic of China
[c] College of Veterinary medicine South China Agricultural University, Guangzhou, People's Republic of China

ARTICLE INFO

Keywords:
Muscovy duck reovirus
Muscovy duckling
Mucosal immune barrier

ABSTRACT

Muscovy duck reovirus (MDRV) causes serious immunodeficiency in the intestinal mucosa, although the underlying histopathological mechanisms remain unclear. Thus, we investigated the impact of MDRV infection on intestinal morphology using hematoxylin and eosin staining. Immune-related cells were also quantified by staining with hematoxylin and eosin, toluidine blue, and periodic acid-Schiff stain, or by immunohistochemistry and cytochemistry for lectin. Similarly, $CD4^+$ and $CD8^+$ cells were quantified by flow cytometry, and the expression of several immune-related molecules was quantified by radioimmunoassay. We found that MDRV clearly damaged the intestinal mucosa, based on tissue morphology, villus length, villus width, intestinal thickness, villus height/crypt depth ratio, and villus surface area. MDRV also altered the density or distribution of lymphocytes, mastocytes, and goblet cells in the small intestinal mucosa, as well as microfold cells in Peyer's patches. In addition, MDRV markedly depleted $CD4^+$ cells from the intestinal mucosa and lowered the $CD4^+$:$CD8^+$ ratio in peripheral blood. Moreover, MDRV diminished the levels of secretory IgA and mucosal addressin cell adhesion molecule-1 ($p < 0.01$), but elevated those of histamine and nitric oxide ($p < 0.01$ or $p < 0.05$). Finally, MDRV significantly suppressed IL-1β, IL-4, IL-5, and IL-8 levels ($p < 0.01$ or $p < 0.05$) mid-infection. Collectively, our data suggest that MDRV severely damages the structure and function of the intestinal mucosa by modulating immune cells and immune-related factors, thus leading to local immunodeficiency. Our findings lay the foundation for further research on the pathogenesis of MDRV.

1. Introduction

Muscovy duck reovirus (MDRV), an *Orthoreovirus,* belonging to the *Reoviridae* family, is highly pathogenic to waterfowl, especially Muscovy ducklings, and causes significant economic losses threats the poultry industry worldwide (Wang et al., 2012). The primary site of MDRV infection is the mucous membrane, where local immunity is subsequently impaired. However, there is limited knowledge regarding the relevance between MDRV and mucosal immune barrier.

The mucosal (epithelial) barrier is generally considered to be the first line of defense against most intestinal bacterial and viral pathogens (Martens et al., 2018). Steady-state maintenance of the barrier function is performed by immune-related cells of the intestinal mucosal epithelium. The barrier consists of Peyer's patches and they are diffuse lymphoid tissues that are effector sites that trigger an immune response (Allaire et al., 2018). Peyer's patches are enriched in microfold cells, a form of specialized epithelial cells (Ohno, 2016). The intestinal epithelial cells play a important role in transmitting signals, presenting antigens, and mounting multiple immune responses, enhancing antiviral protection (Pervolaraki et al., 2017). In addition, intestinal epithelium is the main gathering place of T cells (Huang et al., 2016). Various immune-related cells are also present in the gut epithelium, including lymphocytes, mast cells, and goblet cells, which secrete an array of cytokines and immunoglobulins, altering the extracellular environment (Robertson et al., 2018). Although a successful adaptive immune response depends on humoral and cellular immunity, as well as appropriate interactions between them, intestinal mucosal immunity is also related to humoral (Guardiola et al., 2018). Therefore, it can be

* Corresponding author.
E-mail address: zjhyfang@163.com (Y. Huang).
[1] These authors contributed equally to this work and should be regarded as co-first authors.

https://doi.org/10.1016/j.vetmic.2019.04.017
Received 14 November 2018; Received in revised form 4 April 2019; Accepted 11 April 2019

assessed by quantifying lymphocytes, cytokines and immunoglobulins. MDRV has been shown to seriously damage the mucosa (Jiang et al., 2015), thus, the mucosal immunity of ducks to MDRV should also be studied.

In this study, we investigated the effect of MDRV on intestinal mucosal immunity based on the changes in intestinal tissue morphology and function, including immune-related cells (intraepithelial lymphocytes, microfold cells, mast cells, goblet cells, $CD4^+$ and $CD8^+$ cells), as well as changes in secretory IgA , mucosal address in cell adhesion molecule-1 (MAdCAM-1), histamine, NO, and interleukins in muscovy ducklings. The data advance our understanding of the potential mechanisms driving intestinal mucosal immune deficiency during MDRV infection.

2. Materials and methods

2.1. MDRV strain and animals

The YB strain was isolated and is archived in our laboratory (Wu et al., 2001). Healthy 1-day-old Muscovy ducklings that were free of MDRV were purchased from a farm in Putian (Fujian, China).

2.2. Infection

As described previously (Wu et al., 2018), 100 healthy Muscovy ducklings were divided randomly (n = 50/group) into a control group, and a test group. The test group (n = 50) was exposed to the ducklings (n = 20) intramuscularly infected with 2000 $TCID_{50}$ of MDRV, resulting in infection of as a result of contact transmission. All animals were cared for according to the International Guiding Principles for Biomedical Research Involving Animals, issued by the Council for the International Organizations of Medical Sciences. Six ducklings each from the control or infected cohorts were sacrificed at 1, 3, 6, 10, 15, and 21 days post-infection (dpi) for tissue collection and analysis.

2.3. Quantitative RT-PCR

MDRV load was monitored by quantitative RT-PCR of the p10 gene. Briefly, total RNA was extracted from the duodenum using TransZol Up Plus RNA Kit (TransGen, Beijing, China), following the manufacturer's instructions. cDNA was generated with PrimeScript™ RT Master Mix (TaKaRa, Dalian, China), and targets were amplified in triplicate using SYBR Premix DimerEraser™ (TaKaRa, Dalian, China), on a Bio Rad CFX Connect™ Real Time PCR Detection System (Bio Rad Hercules, CA, USA). p10 was amplified using 5′- CGTGTCCTGTCGGTCTTAGC-3′ and 5′- TGAAGGTGGTATTCGTTCCAG-3′, whereas GAPDH was amplified using 5′-TGCTAAGCGTGTCATCATCT-3′ and 5′-AGTGGTCATAAGACC CTCCA-3′. Reaction parameters were set according to the manufacturer's instructions. p10 expression was quantified by the $2^{-\Delta\Delta Ct}$ method and normalized to that of GAPDH.

2.4. Histology

Seventy-two duodenum, jejunum, and ileum segments were immediately fixed in 4% paraformaldehyde in 0.1 M phosphate-buffered saline (pH 7.4, 4 °C) for 48 h and embedded in paraffin for sectioning (5 μm, cross-section). The tissue sections were stained with hematoxylin-eosin (HE), periodic acid-Schiff (PAS) and Toluidine Blue Staining (TBS). At least 60 random fields in six sections of each sample were photographed at 400 × magnification with a microscope (BX51; Olympus, Tokyo, Japan). The five longest villi per view and a total of 300 longest villi (in each sample) were analyzed per treatment. The villus length (V), crypt depth (C) and crypt depth and villus length/crypt depth (V/C) ratio from HE-staining, the number of goblet cells per 100 absorb cells from PAS-staining and the number of mast cells per mm^2 from TB-staining were measured.

2.5. Immunohistochemistry

Sections were incubated overnight at 4 °C with the monoclonal rabbit anti-mouse antibodies (microfold cells, 1:200; Abcam, Cambridge, MA, USA). The sections were subsequently rinsed with 0.01 M PBS (pH 7.4) and incubated with biotinylated goat anti-rabbit IgG (1:200; Sigma, St. Louis, MO) for 2 h at room temperature. After washing, the tissues were incubated with streptavidin-horseradish peroxidase (1:250, Sigma, St. Louis, MO) for 2 h at room temperature. Immunoreactivity was visualized by incubating the tissue sections in 0.01 M PBS that contained 0.05% 3′, 3-diaminobenzidine tetrahydrochloride (DAB; Sigma, St. Louis, MO) and 0.003% hydrogen peroxide for 10 min in the dark. The sections were then stained with hematoxylin and mounted. Negative control slides without the primary antibody were examined in all cases. Immunoreactive cells were presented with yellow brown staining in the cell. The positive cells were counted in 25 random fields from five cross-sections in each sample. The mean integral optical density (IOD) of the positive cells was determined.

2.6. Cytology

Lymphocytes (n = 6/group) were separated from peripheral blood using Duck Peripheral Blood Lymphocyte Separator Kit (TBD, Tianjin, China, LTS1090D) and resuspended in 500 μL of pre-cooled PBS containing 10% fetal bovine serum and 1% sodium azide, resulting in suspensions with 1~2 × 10^6 lymphocytes/mL. Of these, 100 μL samples were probed for 30 min at 4 °C and in the dark with 0.1–10 μL of rat monoclonal antibodies to duck $CD4^+$ (AbD Serotec, Kidlington, UK) and $CD8^+$ (AbD Serotec, Kidlington, UK) diluted in 2% bovine serum albumin in PBS. Samples were then labeled for 30 min at 4 °C and in the dark with goat anti-rat IgG conjugated to FITC (TransGen, Beijing, China), also diluted in 2% bovine serum albumin in PBS. Finally, samples were washed with 1 mL PBS, resuspended in 500 μL of pre-cooled PBS containing 10% fetal bovine serum and 1% sodium azide, and analyzed on a FACS Canto II Flow Cytometer (BD, Beijing, China).

2.7. Radioimmunoassay

10 cm tissue sections (n = 6/group)were collected from the duodenum jejunum and ileum, washed with pre-cooled sterile PBS and dried on neutral filter paper, then weighed. Mucus was collected into an eppendorf tube containing 1 mL 0.01 mol/L PBS, then washed and centrifuged it for 15 min at 4 °C, 3000 rpm. Secretory IgA, MAdCAM-1, histamine, NO, and interleukins were quantified using radio immunological kits (Huaying Biotechnology Research Institute, Beijing, China). The resulting supernatant was collected, and assayed for total protein using Bradford brilliant blue. Secretory IgA, MAdCAM-1, histamine, NO, and interleukins were then quantified by double antibody sandwich RIA (Sinouk, Beijing, China) using samples containing 1 mg total protein. All other chemicals used in this study were analytical grade.

2.8. Statistical analysis

Data are expressed as the mean ± standard deviation and were analyzed using SPSS 17.0 statistical software (SPSS, Inc., Chicago, IL, USA). Differences between groups were statistically analyzed using ANOVA followed by One-way ANOVA, which were used to determine the significance of differences among groups ($p < 0.05$ and $p < 0.01$).

3. Results

3.1. Dynamics of MDRV infection in duodenum mucosa

As assessed by quantitative RT-PCR, mRNA levels of the MDRV p10

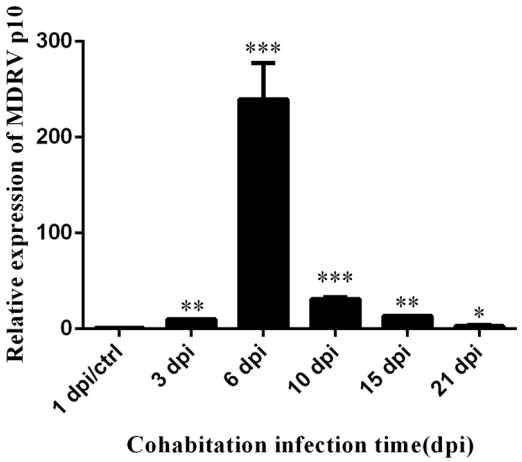

Fig. 1. Dynamics of MDRV infection in duodenum mucosa. Duodenum tissues were collected from infected and uninfected ducklings (n = 6/group) at 1, 3, 6, 10, 15, and 21 days post-infection, and analyzed by real time PCR for MDRV mRNA. Samples were tested in triplicate. **, $p < 0.01$; *, $p < 0.05$ vs uninfected ducklings.

gene significantly increased ($p < 0.05$) at 3, 6, 10, 15, and 21 days post-infection, relative to levels at 1 day post-infection (Fig. 1). These mRNA levels peaked at 6˜10 days post-infection, but expression was undetectable in mock-infected ducklings.

3.2. MDRV degrades the small intestinal mucosa

As shown by hematoxylin and eosin staining in Fig. 2A, the intestinal mucosa in mock-infected Muscovy ducklings was structurally intact, with orderly villi and without evidence of congestion, edema, abnormal epithelial cells, or infiltration by inflammatory cells. In contrast, the intestinal mucosal villi of MDRV-infected Muscovy ducklings were loose, atrophic, and necrotic, and showed shedding, leading to exposure of the lamina propria. Epithelial cells were also necrotic, while the mucosa, serosa, and myometrium were edematous and infiltrated with inflammatory cells. Lymphocyte nuclei were heavily stained (Fig. 2A). Further studies showed that MDRV not only inhibited the migration of intraepithelial lymphocytes and goblet cells to the top of the villus epithelium, but also depleted these cells from the basement membrane (Fig. 2A,B). Additionally, goblet cells were insufficiently differentiated, as indicated by cellular shrinkage and incomplete staining (Fig. 2B). As shown in Fig. 2C, mast cells were also smaller, with connective tissue significantly depleted from the middle axis of the villus. Finally, microfold cells were not clearly visible, and villi and Peyer's patches were incompletely developed (Fig. 2D). Collectively, the results suggest that MDRV severely degrades the morphological structure of the small intestinal mucosa.

Important indicators of intestinal function, namely villi length, villi width, V/C ratio, villus surface area, and thickness of the duodenum, jejunum, and ileum were all significantly lower ($p < 0.05$ or $p < 0.01$) at 3, 6, 10, 15, and 21 days post-infection, except for villi length in the ileum and villi width in the duodenum at 3 days post-infection (Fig. 3). These results imply that MDRV infection significantly alters intestinal parameters, probably promoting intestinal dysfunction and immunosuppression as a result.

3.3. MDRV diminishes immune-related cells in the small intestinal mucosa and alters T cell subsets in peripheral lymphoid blood

In comparison to uninfected ducklings, lymphocytes and goblet cells accumulated in the intestinal mucosa 3 days post-infection, but significantly diminished ($p < 0.01$) thereafter (Fig. 4A,B), as assessed by cell-specific staining. Meanwhile, mastocytes significantly diminished throughout the infection (Fig. 4C). In addition, flow cytometry showed that $CD4^+$ T lymphocytes in peripheral lymphoid blood significantly accumulated ($p < 0.01$) at 3 days post-infection before diminishing ($p < 0.01$), although the loss of $CD8^+$ T cells was not significant except at 10 days post-infection. Accordingly, the $CD4^+$:$CD8^+$ ratio followed the same trends as those of $CD4^+$ T lymphocytes (Fig. 4D). Microfold cells in Peyer's patches were remarkably diminished ($p < 0.05$ or $p < 0.01$) at 15 and 21 days post-infection (Fig. 4E). Taken together, the results indicate that MDRV represses cellular immunity by depleting immune-related cells at the intestinal mucosal barrier, and by diminishing $CD4^+$ cells and lowering the $CD4^+$:$CD8^+$ ratio in peripheral lymphoid blood.

3.4. MDRV infection regulates secretory IgA, MAdCAM-1, histamine, and NO production

Secretory IgA significantly diminished ($p < 0.01$) in the small intestinal mucosa at all post-infection time points studied compared to levels in control ducklings (Fig. 5A). On the contrary, MAdCAM-1 significantly accumulated ($p < 0.01$) at 1 and 3 days post-infection, but its levels diminished ($p < 0.01$) at 6 days post-infection (Fig. 5B). Further, intestinal histamine and NO clearly accumulated at 3, 6, 10, 15, and 21 days post-infection (Fig. 5C,D). Similarly, MDRV significantly boosted IL-6 production at 3 days post-infection, and suppressed IL-1β, IL-4, IL-5, and IL-8 levels mid-infection (6–10 days post-infection), but not the levels of IL-6 and IL-15. In late infection (21 days post-infection), MDRV also significantly suppressed IL-5 levels, while markedly elevating IL-8 and IL-15 levels (Fig. 5E–J). These results imply that secretory IgA, MAdCAM-1, histamine, NO, and interleukins likely regulate intestinal mucosal immunity.

4. Discussion

The mechanical barrier (intestinal mucosal epithelia) and immune barrier (gut-associated lymphoid tissue) are the major components of the intestinal barrier (Liu et al., 2009). Integrity of intestinal mechanical barrier (intestinal mucosal epithelia) directly affects barrier and absorptive functions (Vancamelbeke and Vermeire, 2017). Here we chose to examine a MDRV contact-infected Muscovy duck model to explore the effects of MDRV on injury of the intestinal barrier and intestinal immune function. Results showed that MDRV significantly decreased the villi width, intestinal thickness, V/C ratio, and villus surface area ($p < 0.05$ or $p < 0.01$), causing loss of absorptive and barrier functions, and further resulting in a higher mortality rate of infected Muscovy ducklings and blocked growth of surviving ducklings after infection.

What is the cause of damage to the intestinal structure caused by MDRV infection? We further examined changes in intestinal immune-related cells and cytokines following MDRV infection.

Intraepithelial lymphocytes (IELs) are perfectly positioned within the intestinal epithelium to provide the first line of mucosal defense against luminal microbes or rapidly respond to epithelial injury (Patterson and Watson, 2018). In our study, MDRV obviously inhibited the migration of IELs to the top of the epithelial cells and depleted $CD4^+$ T cells of IELs from the gut mucosa, resulting in significantly lower $CD4^+$: $CD8^+$ ratio, which is typically used as an index to follow long-term immunity and to monitor both immune dysfunction and viral reservoir size (Hughes et al., 2018). Thus, impaired immunity of IELs is likely an important driver of immunosuppression in the intestinal mucosa. Moreover, directional migration of immune cells is a prerequisite for immune response, and migration of T and B cells to the gut is generally facilitated by the interaction of α4β7 integrin and its ligand MAdCAM-1 (Clahsen et al., 2015). We found that MAdCAM-1 significantly accumulates in early MDRV infection, probably lead to lymphocytes homing to the gut to mount an immune response. Strikingly, progression of MDRV infection further compromises adaptive and

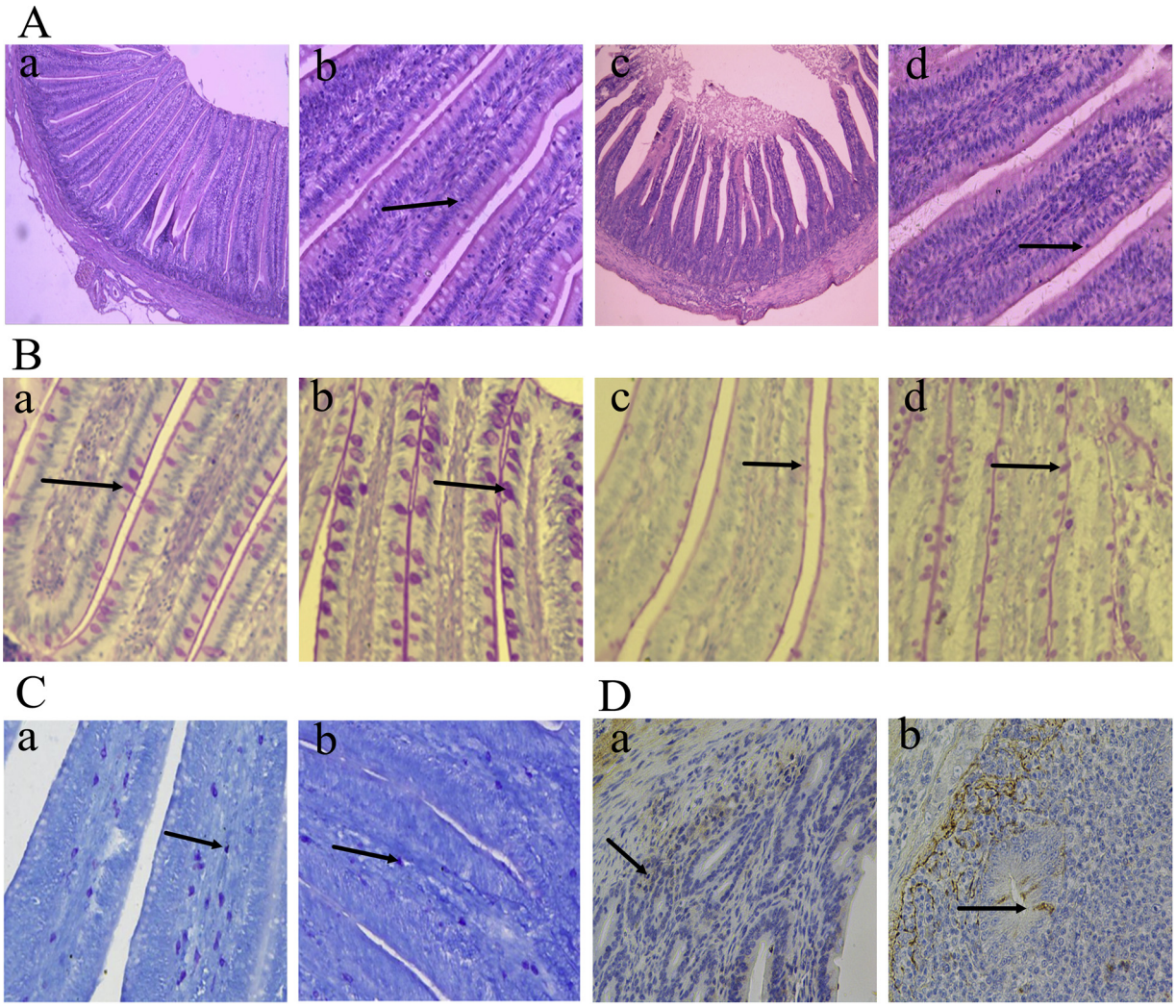

Fig. 2. Effects of MDRV on morphology of the duodenum. Small intestines were obtained at 15 days post-infection were sectioned, stained, and examined under a TESA ETALON TCM 100 light microscope (Switzerland). (**A**) Hematoxylin and eosin staining for observation of lymphocytes in control (a, b) or MDRV-infected group. Panels a and c are 100×, panels b and d are 400 × . (**B**) Periodic acid-Schiff staining for observation of goblet cells in control (a, b) or infected ducklings (c, d), 400 × . (**C**) Toluidine blue staining for observation of mast cells in control (a) or infected ducklings (b), 400 × . (**D**) Immunohistochemical and lectin cytochemical staining for observation of microfold cells in control (a) or infected ducklings (b), 400 × (For interpretation of the references to colour in this figure legend, the reader is referred to the web version of this article).

mucosal immunity, leading to further loss of MAdCAM-1 at late stages of infection (6˜21 dpi), which decrease lymphocytes homing. In addition, MDRV can induce the higher apoptosis rate of lymphocytes, especially in 9 dpi ~ 12 dpi (Luo et al., 2019). Therefore, we speculate that MDRV infection induces lymphocyte apoptosis and the reduction of lymphocyte homing as causes of intestinal mucosal lymphopenia in MDRV-infected ducklings.

Goblet cells are also important immunocytes and are able to secrete intestinal mucus containing intestinal trefoil factor (TFF3) as a diffuse barrier protecting the intestinal mucosal epithelium, which is essential in maintaining mucosal integrity in gastrointestinal tract (Gibbins et al., 2015). Our results showed that, in the middle and late period of MDRV infection (6˜21 dpi), MDRV caused remarkable decrease of goblet cells number at the upper region of the duodenal villi, as well as cellular shrink and unclear staining with light red. Mast cells are not only the effector cells in native immunity, but also participate in acquired immunity, which are the first-line cells for anti-infection immunity. Upon contacting with the exogenous antigens, mast cells can quickly and selectively produce active mediators to trigger protective immune responses (Ohno, 2016). And evidences have revealed that functional enhancement of mast cells can up-regulate the body's anti-virus ability. Our results showed that late infection of MDRV caused remarkable decrease of mast cells counts and cellular shrink in lamina propria of duodenal mucosa, which suggested that MDRV inhibited the growth and development of mast cells, and brought damages to intestinal native and acquired immune response.

Microfold cells of the Peyer's patches are a special kind of intestinal epithelium mucosa cell that can collect granular antigens and pass them to DCs and macrophages, which can then activate the T cells (Otsuka and Kabashima, 2015). The activated T cells will further activate B cells and the latter will produce antigen-specific secretory IgA after homing to the effector site. Of note, secretory IgA is the first line in the fight of body against the enteroviruses and respiroviruses in mucosal immunity (Mora and von Andrian, 2008). In our study, we found that MDRV depleted microfold cells and secretory IgA, indicating that MDRV disrupted the function of intestinal mucosal antigen capture and recognition in Muscovy ducklings, and resulting in a decrease or inactive activity of immune cells who secretory IgA. Eventually it leads to intestinal mucosal immune function inactivation.

At the same time, histamine significantly accumulates in the gut of infected Muscovy ducklings, possibly causing damage or inflammation or necrosis of intestinal tissue by altering cell excitability and regulating

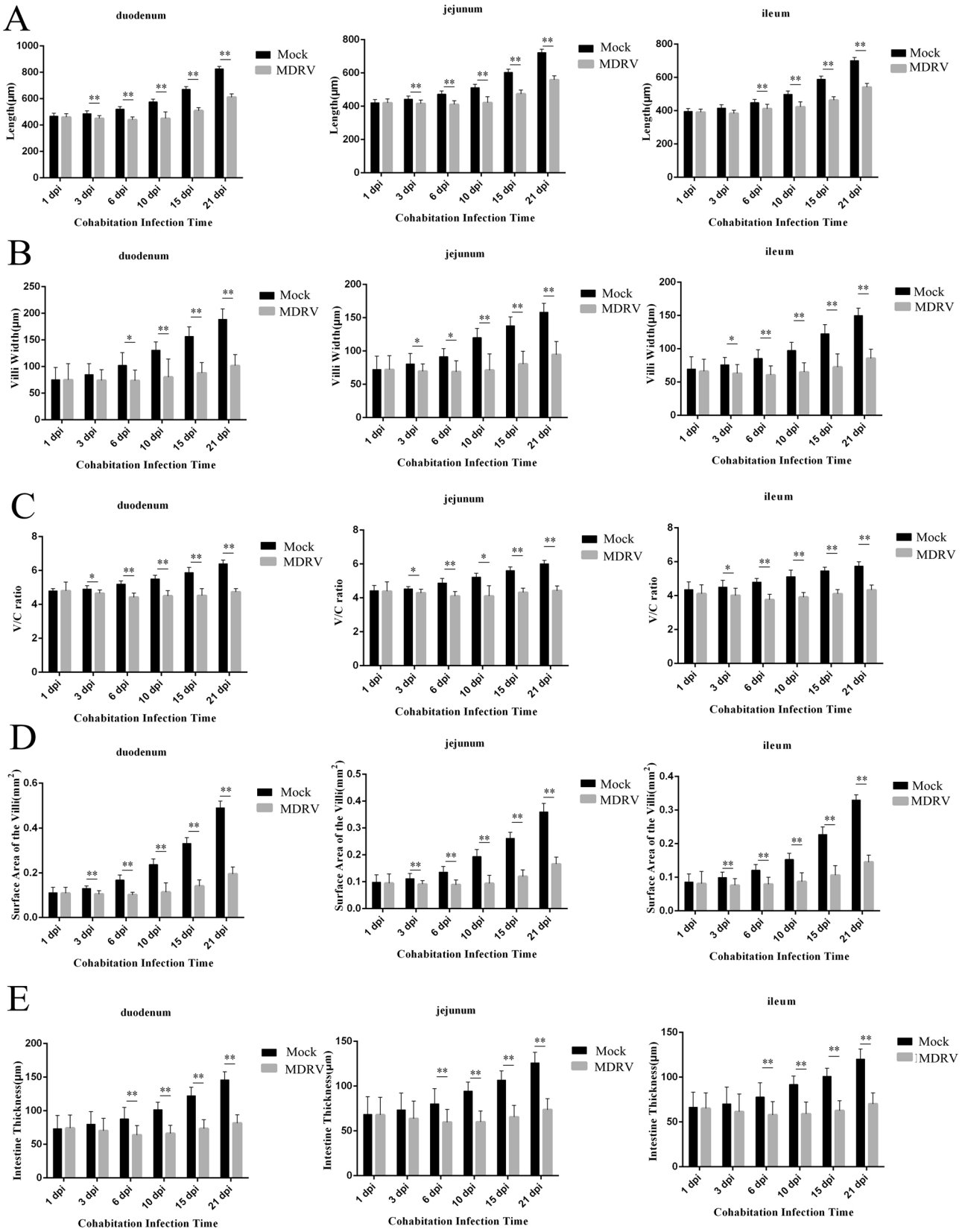

Fig. 3. Effects of MDRV on histological features of the duodenum, jejunum, and ileum. Small intestines were collected at 1, 3, 6, 10, 15, and 21 days post-infection, sectioned, stained with hematoxylin and eosin, and examined at 400× on a TESA ETALON TCM 100 light microscope (Switzerland) to assess changes in (**A**) villi length, (**B**) villi width, (**C**) villus height/crypt depth ratio, (**D**) villus surface area, and (**E**) thickness. **, $p < 0.01$; *, $p < 0.05$ vs uninfected ducklings.

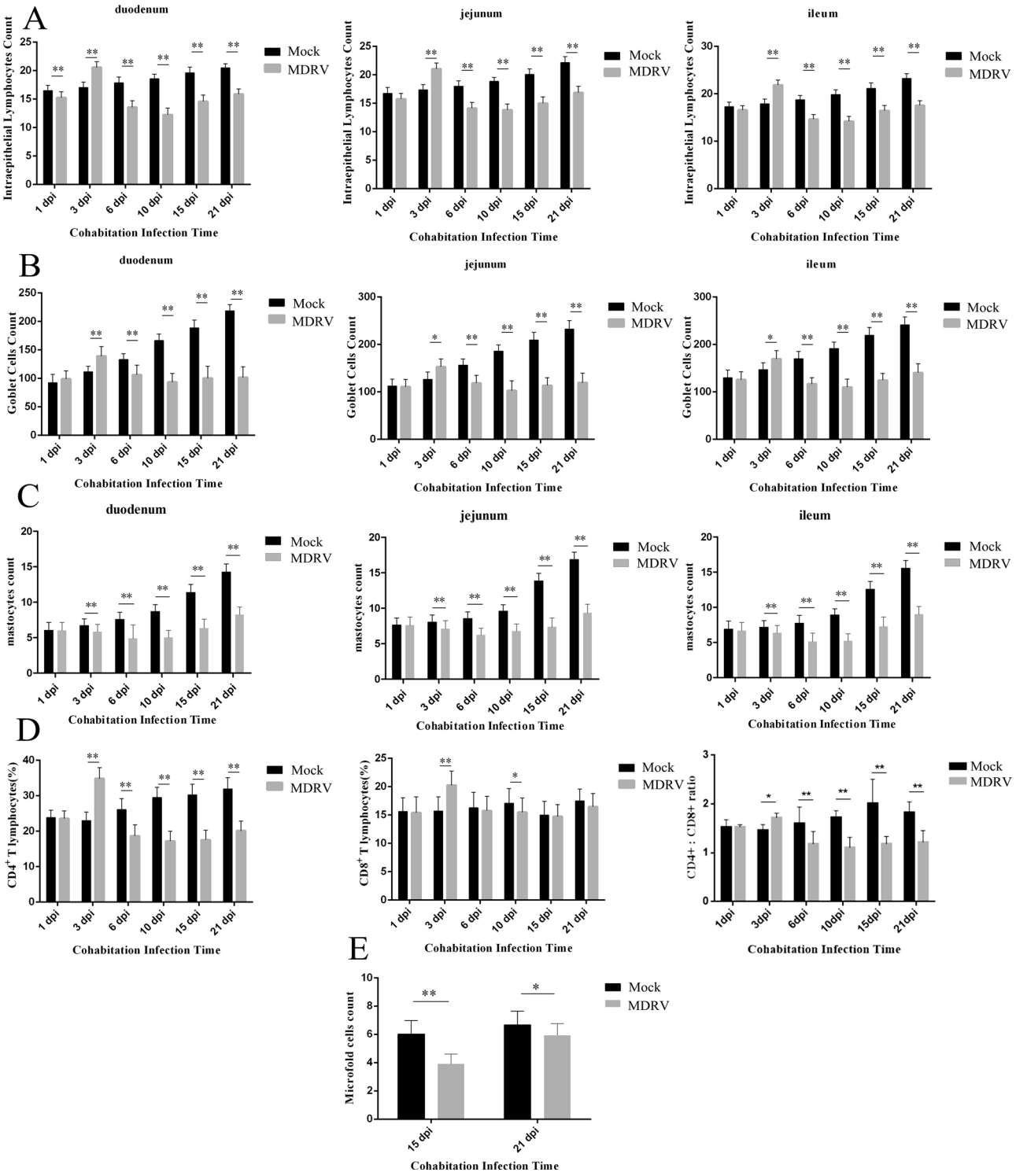

Fig. 4. Effects of MDRV on immune-related cells in the intestinal mucosa and peripheral blood. Small intestines from uninfected and infected ducklings were obtained at 1, 3, 6, 10, 15, and 21 days post-infection, sectioned, stained with hematoxylin and eosin, and examined at 400× on a TESA ETALON TCM 100 light microscope (Switzerland) to determine the average number of immune cells per visual field (0.01 mm^2). (**A**) Intraepithelial lymphocytes, (**B**) goblet cells, and (**C**) mast cells in the duodenal, jejunum, and ileum endothelium. (**D**) $CD4^+$ cells, $CD8^+$ cells, and $CD4^+$:$CD8^+$ ratio in peripheral blood, as assessed by flow cytometry. (**E**) microfold cells in Peyer's patches. microfold cells were not enumerated at time points that are not shown due to incomplete development of Peyer's patches. **, $p < 0.01$; *, $p < 0.05$ vs uninfected ducklings.

the interaction between cytokines (Cilz and Lei, 2017). NO is a key mediator of numerous physiological and pathological systems (Schairer et al., 2012). Constitutively low levels of NO can reduce inflammation and repair of damaged tissue, while higher concentrations of NO most often giving rise to opposite outcomes (Lin et al., 2007; Vieira and Kroemer, 2003). MDRV promotes boosts NO production in the intestine, inhibiting mitochondrial function and causing apoptosis, an increase in intestinal epithelial permeability and decreased intestinal barrier function. Interleukins belong to a large class of cytokines, which are secreted by various host cells to regulate multiple processes (Zhao

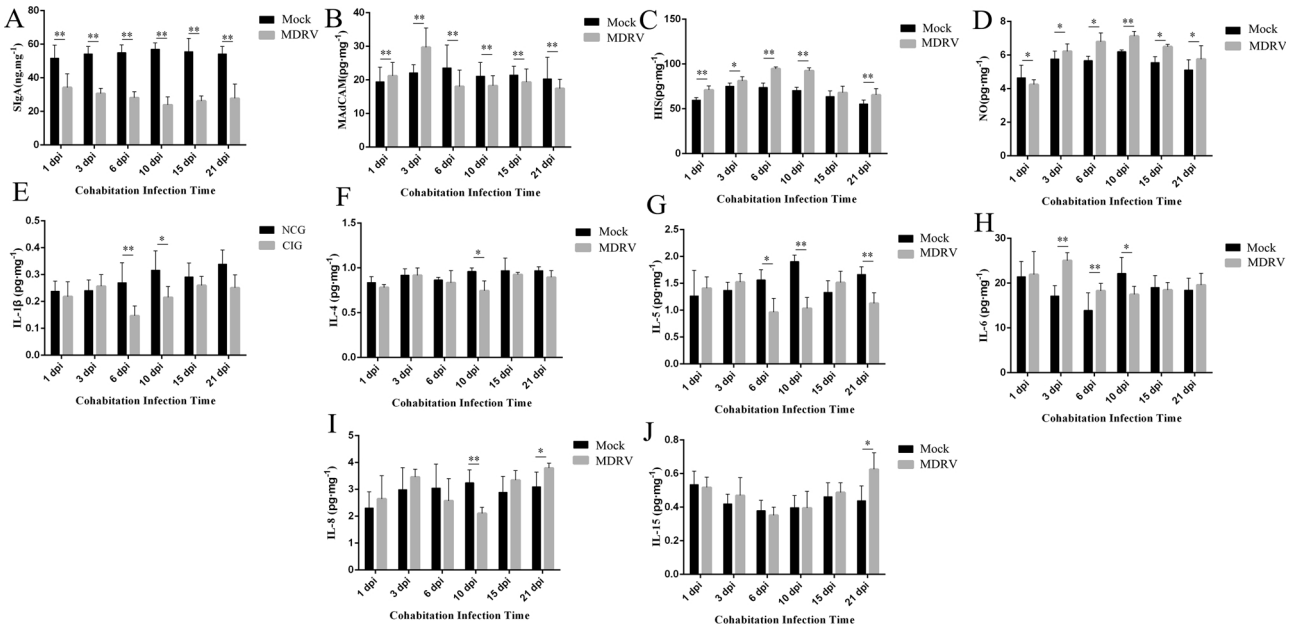

Fig. 5. Effects of MDRV on the secretion of duodenum cytokines (Secretory IgA, MAdCAM-1, histamine, NO and interleukins). (A) secretory IgA, (B) MAdCAM-1, (C) histamine, (D) NO, (E) IL-1β, (F) IL-4, (G) IL-5, (H) IL-6, (I) IL-8, and (J) IL-15 were measured by radioimmunoassay (n = 3/group). **, $p < 0.01$; *, $p < 0.05$ vs uninfected ducklings.

et al., 2015). In the mid-infection (6˜10 dpi), MDRV broadly suppresses the production of pro-inflammatory (IL-1β, IL-8, IL-15) and anti-inflammatory cytokines (IL-4, IL-5), which caused by a large decrease in the number of immune-related cells in the intestinal mucosa. It is indicated that MDRV inhibits the proliferation of intestinal B lymphocytes and mast cells, and also inhibits the activity of T lymphocytes and the function of macrophages and lymphocyte migration (Curfs et al., 1997; Lin et al., 2000). In the early stage of MDRV infection (1dpi˜3 dpi), the rapid increase of some immune cell numbers and cytokines in the intestine of Muscovy ducklings may be the main factor leading to intestinal inflammation, such as IL-6.

Taken together, our results suggest that MDRV infection induces a large reduction in immune-related cells on the intestinal mucosa, resulting in destruction of intestinal mucosal structures and imbalance in cytokines, It eventually leads to intestinal mucosal immune dysfunction. Our results will lay the foundation for further study of the pathogenesis and mucosal immune mechanisms of MDRV-infected ducklings.

Ethics approval

The animal protocols used in this work and all procedures of the experiment were performed in compliance with the laws and guidelines of the Fujian Agricultural and Forestry University Animal Care and Use Committee (Approval No: PZCASFAFU201604)

Conflict of interest statement

The authors declare no conflict of interest

Acknowledgments

This research was supported by the College of Animal Sciences FAFU (Grant Number: 2018K005), the Natural Science Foundation of China (Grant Number: 31372474), and the Natural Science Foundation of Fujian Province (Grant Number: 2017J01597).

References

Allaire, J.M., Crowley, S.M., Law, H.T., Chang, S.Y., Ko, H.J., Vallance, B.A., 2018. The intestinal epithelium: central coordinator of mucosal immunity. Trends Immunol. 39, 677–696.

Cilz, N.I., Lei, S.B., 2017. Histamine facilitates GABAergic transmission in the rat entorhinal cortex: roles of H1 and H2 receptors, Na^+-permeable cation channels and inward rectifier K^+ channels. Hippocampus 5, 613–631.

Clahsen, T., Pabst, O., Tenbrock, K., Schippers, A., Wagner, N., 2015. Localization of dendritic cells in the gut epithelium requires MAdCAM-1. Clin. Immunol. 156, 74–84.

Curfs, J.H., Meis, J.F., Hoogkamp-Korstanje, J.A., 1997. A primer on cytokines: sources, receptors, effects, and inducers. Clin. Microbiol. Rev. 10, 742–780.

Gibbins, H.L., Proctor, G.B., Yakubov, G.E., Wilson, S., Carpenter, G.H., 2015. sIgA binding to mucosal surfaces is mediated by mucin-mucin interactions. PLoS One 10, e119677.

Guardiola, F.A., Barroso, C., Enes, P., Couto, A., Díaz-Rosales, P., Afonso, A., Kanashiro, E., Peres, H., Matos, E., Oliva-Teles, A., Pousão-Ferreira, P., Costas, B., 2018. Humoral and mucosal immune responses in meagre (*Argyrosomus regius*) juveniles fed diets with varying inclusion levels of carob seed germ meal. Fish Shellfish Immunol. 79, 209–217.

Huang, Y.F., Wu, Y.J., Li, Y.C., Jiang, H., Huang, L., Huang, S., Chen, J., Sun, X., 2016. Relationship between intestinal tract restoration by *Hericium erinaceus* polysaccharide and MAdCAM-1 secretion in MDRV-infected Muscovy ducklings. China Poult. VV.

Hughes, R.A., May, M.T., Tilling, K., Taylor, N., Wittkop, L., Reiss, P., Gill, J., Schommers, P., Costagliola, D., Guest, J.L., Lima, V.D., d'Arminio Monforte, A., Smith, C., Cavassini, M., Saag, M., Castilho, J.L., Sterne, J.A.C., 2018. Long terms trends in $CD4^+$ cell counts, $CD8^+$ cell counts, and the $CD4^+$:$CD8^+$ ratio. AIDS 32, 1361–1367.

Jiang, H.H., Huang, L.N., Wu, B.C., Li, J., Wu, Y.J., Huang, Y.F., 2015. Effects of *Hericium edodes* polysaccharides on mortality and intestinal morphology of Muscovy duck infected by MDRV. Chin. Poult. VV 22–26.

Lin, E., Calvano, S.E., Lowry, S.F., 2000. Inflammatory cytokines and cell response in surgery. Surgery 127, 117–126.

Lin, S.K., Kok, S.H., Lin, L.D., et al., 2007. Nitric oxide promotes the progression of periapical lesion via inducing macrophage and osteoblast apoptosis. Oral Microbiol. Immunol. 22 (1), 24–29.

Liu, C., Li, A., Weng, Y.B., Duan, M.L., Wang, B.E., Zhang, S.W., 2009. Changes in intestinal mucosal immune barrier in rats with endotoxemia. World J. Gastroenterol. 15, 5843–5850.

Luo, Y., Li, H.W., Liu, Z.N., et al., 2019. Effects of Hericium erinaceus polysauharide on apoptosis of the main immune organs and serum immune-related indexes of Muscovy duckling infected withMuscovy duck reovirus. Zhongguo Shouyi Keji. https://doi.org/10.16656/j.issn.1673-4696.

Martens, E.C., Neumann, M., Desai, M.S., 2018. Interactions of commensal and pathogenic microorganisms with the intestinal mucosal barrier. Nat. Rev. Microbiol. 16, 457–470.

Mora, J.R., von Andrian, U.H., 2008. Differentiation and homing of IgA-secreting cells. Mucosal Immunol. 1, 96–109.

Ohno, H., 2016. Intestinal m cells. J. Biochem. 159, 151–160.

Otsuka, A., Kabashima, K., 2015. Barrier function and cutaneous immunology. Arerugi 64, 1189–1195 (Article in Japanese).

Patterson, A.M., Watson, A.J.M., 2018. Intraepithelial lymphocytes are the first line of defense against enteric infection. Gastroenterology 155, 1640–1642.
Pervolaraki, K., Stanifer, M.L., Münchau, S., Renn, L.A., Albrecht, D., Kurzhals, S., Senís, E., Grimm, D., Schröder-Braunstein, J., Rabin, R.L., Boulant, S., 2017. Type I and type III interferons display different dependency on mitogen-activated protein kinases to mount an antiviral state in the human gut. Front. Immunol. 8, 459.
Robertson, S.J., Goethel, A., Girardin, S.E., Philpott, D.J., 2018. Innate immune influences on the gut microbiome: lessons from mouse models. Trends Immunol. 39, 992–1004.
Schairer, D.O., Chouake, J.S., Nosanchuk, J.D., Friedman, A.J., 2012. The potential of nitric oxide releasing therapies as antimicrobial agents. Virulence 3, 271–279.
Vancamelbeke, M., Vermeire, S., 2017. The intestinal barrier: a fundamental role in health and disease. Expert Rev. Gastroenterol. Hepatol. 11, 821–834.
Vieira, H., Kroemer, G., 2003. Mitochondria as targets of apoptosis regulation by nitric oxide. IUBMB Life 55 (10-11), 613–616.
Wang, D., Xu, F., Ma, G., Zhang, C., Huang, Y., Li, H., Zhang, D., 2012. Complete genomic sequence of a new Muscovy duck-origin reovirus from China. J. Virol. 86, 12445.
Wu, B.C., Chen, J.X., Yao, J.S., Chen, Z.H., Chen, W.L., Li, G.P., Zeng, X.C., 2001. Isolation and identification of Muscovy duck reovirus. J. Fujian Agric. Univ. 30, 227–230.
Wu, Y.J., Jiang, H., Zhu, E.P., Li, J., Wang, Q.X., Zhou, W.D., Qin, T., Wu, X.P., Wu, B.C., Huang, Y.F., 2018. *Hericium erinaceus* polysaccharide facilitates restoration of injured intestinal mucosal immunity in Muscovy duck reovirus-infected Muscovy ducklings. Int. J. Biol. Macromol. 107, 1151–1161.
Zhao, H.Q., Li, W.M., Lu, Z.Q., Sheng, Z.Y., Yao, Y.M., 2015. The growing spectrum of anti-inflammatory interleukins and their potential roles in the development of sepsis. J. Interferon Cytokine Res. 35, 242–251.